Spectrochimica Acta Part A: Molecular and Biomolecular Spectroscopy 105 (2013) 223–228

Contents lists available at SciVerse ScienceDirect

Spectrochimica Acta Part A: Molecular and Biomolecular Spectroscopy

journal homepage: www.elsevier.com/locate/saa

Synthesis, spectral studies and solvatochromism of some novel benzimidazole derivatives – ESIPT process

J. Jayabharathi *, V. Thanikachalam, K. Jayamoorthy, N. Srinivasan

Department of Chemistry, Annamalai University, Annamalainagar 608 002, Tamil Nadu, India

HIGHLIGHTS

- Absorption and emission spectral studies have been carried out.
- HOMO–LUMO – probable charge transfer taking place.
- Formation of the keto-isomer due to ESIPT.
- Competition of intra and intermolecular hydrogen bonding.

GRAPHICAL ABSTRACT

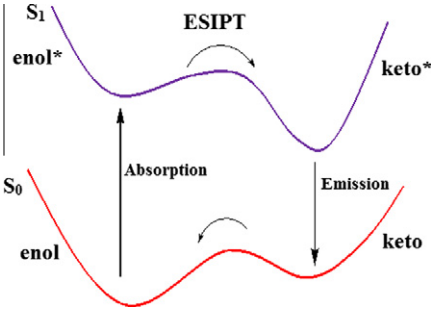

ARTICLE INFO

Article history:
Received 12 October 2012
Received in revised form 2 November 2012
Accepted 11 December 2012
Available online 20 December 2012

Keywords:
Photophysical study
DFT
PES
XRD
ESIPT

ABSTRACT

Some novel benzimidazole derivatives were synthesized and characterized by ^{1}H, ^{13}C NMR mass and elemental analysis. XRD analysis was carried out for 1-(4-methylbenzyl)-2-*p*-tolyl-1H-benzo[d]imidazole. The solvent effect on the absorption and fluorescence bands has been analyzed. The energetic analysis of the potential energy surface (PES), HOMO and LUMO levels [DFT/B3LYP/6-31G(d,p)] evidenced the existence of excited state intramolecular proton transfer (ESIPT) in hydroxy benzimidazole derivative.

Introduction

Heterocyclic imidazole derivatives have attracted considerable attention because of their unique optical properties [1] and used for preparing functionalized materials [2]. Benzimidazole based chromophores have received increasing attention due to their distinctive linear, non-linear optical properties and also due to their excellent thermal stability in guest–host systems [3]. Functionalized benzimidazoles represent an important class of N-containing heterocyclic compounds and have received considerable attention in recent times because of their applications as antiulcer, antihypertensive, antiviral, antifungal, antioxidants and antihistamines among others [4–8]. They are important intermediates in many organic reactions [9,10] and act as ligands to transition metals for modeling biological systems [11,12].

Excited state intramolecular proton transfer (ESIPT) has become a field of active research [13–17] due to the practical applications of ESIPT exhibiting molecules as laser dyes [18], photo stabilizers [19], fluorescent probes in biology [20] and light-emitting materials for electroluminescent devices [21–23]. ESIPT occurs in aromatic molecules having a phenolic hydroxy group with an intramolecular hydrogen bond to the nearby hetero atom of the same chromophore. Mechanism of ESIPT process is currently being used to understand the photophysics of some molecules that show such interesting characteristics as ultraviolet stabilization [24],

* Corresponding author. Tel.: +91 9443940735.
E-mail address: jtchalam2005@yahoo.co.in (J. Jayabharathi).

1386-1425/$ - see front matter © 2012 Elsevier B.V. All rights reserved.
http://dx.doi.org/10.1016/j.saa.2012.12.037

stimulated radiation production [25], information storage [26], fluorescent solar concentrators [27] and environmental probes in biomolecules [28] and organized assemblies [29]. ESIPT process in electronically excited singlet states can be easily recognized by the appearance of a second band to the red of the normal band in the fluorescence spectrum. Normal band is due to emission from S1 state of the molecule in the form which is thermodynamically most stable in S0 state and second band is due to emission from tautomer, formed by ESIPT. In this paper we have reported synthesis, characterization, solvatochromism and ESIPT process of some benzimidazole derivatives.

Experimental

Spectral measurements

The ultraviolet–visible (UV–vis) spectra of the benzimidazole derivatives were measured in an UV–vis spectrophotometer (Perkin Elmer Lambda 35) and corrected for background absorption due to solvent. Photoluminescence (PL) spectra were recorded on a (Perkin Elmer LS55) fluorescence spectrometer. NMR spectra were recorded on Bruker 400 MHz NMR spectrometer. Mass spectra were recorded on a Varian Saturn 2200 GCMS spectrometer.

General procedure for the synthesis of benzimidazole derivatives

A mixture of corresponding aldehyde (2 mmol), *o*-phenylenediamine (1 mmol) and ammonium acetate (2.5 mmol) has been refluxed at 80 °C in ethanol. The reaction was monitored by TLC and purified by column chromatography using petroleum ether:-ethyl acetate (9:1) as the eluent. The chemical structures of all benzimidazoles have been provided in Fig. 1.

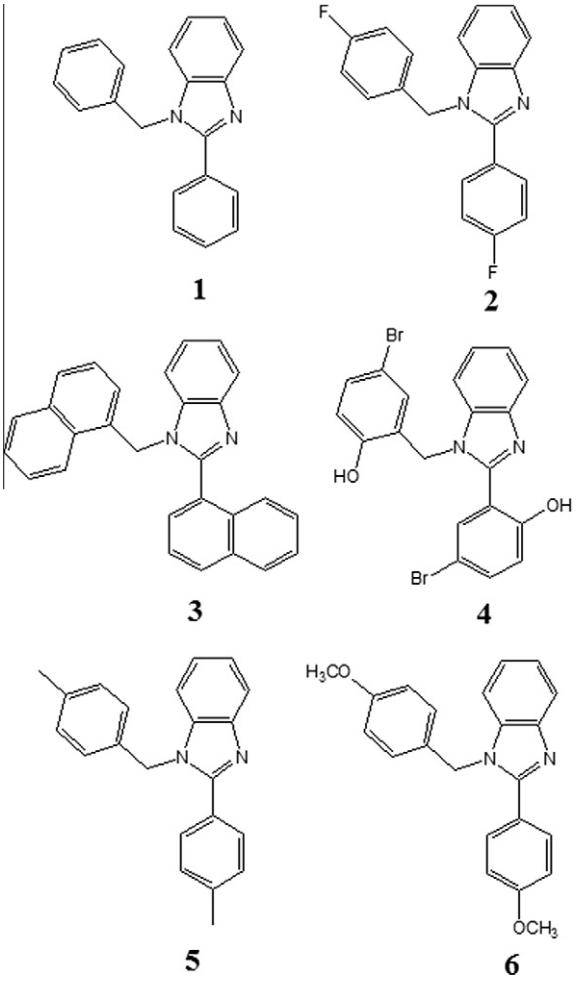

Fig. 1. Chemical structures of benzimidazole derivatives **1**–**6**.

Results and discussion

Absorption and emission spectra of benzimidazole derivatives

Figs. 2 and 3 show the absorption spectrum and emission spectra of benzimidazole derivatives (**1**–**6**) respectively (Table 1). The bathochromic shifts were observed in the fluorescence band of the benzimidazole derivatives with increasing the solvent polarity. Because the distortion of the geometry in the excited state implies a decrease in the resonance energy, the fluorescence band is bathochromically shifted to a higher extent. Moreover, the loss of planarity in the excited state of the benzimidazole derivative could explain the lower fluorescence quantum yield in apolar solvents owing to an increase in the non-radiative processes. However, the shape of the absorption band is independent of the imidazole concentration suggesting the poor aggregation and it is a suitable behavior in the performance of active media of lasers. Indeed, high concentration is necessary to bring about laser action, and the presence of aggregates could drastically reduce the fluorescence quantum yield owing to the efficient quenching of the monomer fluorescence by the aggregates. However, experimental data indicate that the fluorescence band is shifted to lower energies by increasing the concentration. This bathochromic shift is attributed to reabsorption and reemission phenomena [30] and this result corroborates the importance of registering photophysical properties in dilute solutions.

ESIPT process

The fluorescence spectra of **4** in dioxane display an abnormal Stokes-shifted emission band at 329.3 nm and one small shoulder peak at 346.8 nm. Excitation of isomer I lead to the formation of keto-isomer II (Fig. S1) due to ESIPT (Fig. 4).

However in hydroxylic solvent (EtOH), a short wavelength emission band appears for **4** which is absent in the fluorescence spectra of **1**, **2**, **3**, **5** and **6** (Fig. 3). This result corresponds to the results obtained earlier for compounds demonstrating ESIPT [31,32]. Absence of dual emission in these compounds explained by the presence of intermolecular hydrogen bonding with solvent molecule leading to the stabilization of solvated isomer III in which ESIPT is impossible.

Existence of ESIPT mechanism in hydroxy benzimidazole derivative (**4**) was supported by DFT calculation. The electron density of keto and enol isomers of **4** in the ground and excited states calculated by B3LYP/6-31G(d,p) method was tabulated (Table 2). Excitation of enol isomer leads to increase the electron density at N(15) nitrogen atom and decreases the same at oxygen atom resulting in ESIPT. As a consequence of ESIPT, excited keto isomer is formed. The excited keto isomer emits luminescence and returns to ground state keto form (III). This is characterized by a large positive charge at N(15) nitrogen atom and negative charge at oxygen atom. As a result, a reverse process occurs in ground state of the molecule producing enol form.

Driving force for ESIPT process

The existence of intramolecular hydrogen bond in hydroxy benzimidazole **4** is confirmed by the presence of the singlet at

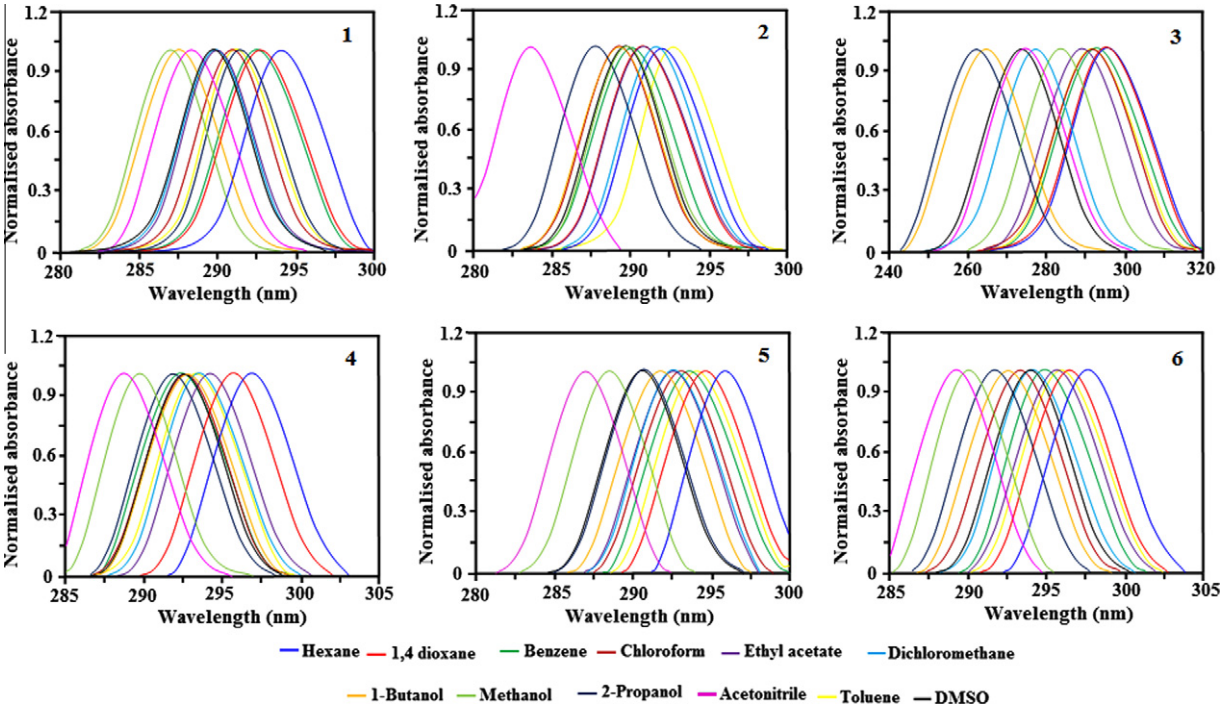

Fig. 2. Absorption spectra of the benzimidazole derivatives **1**–**6**.

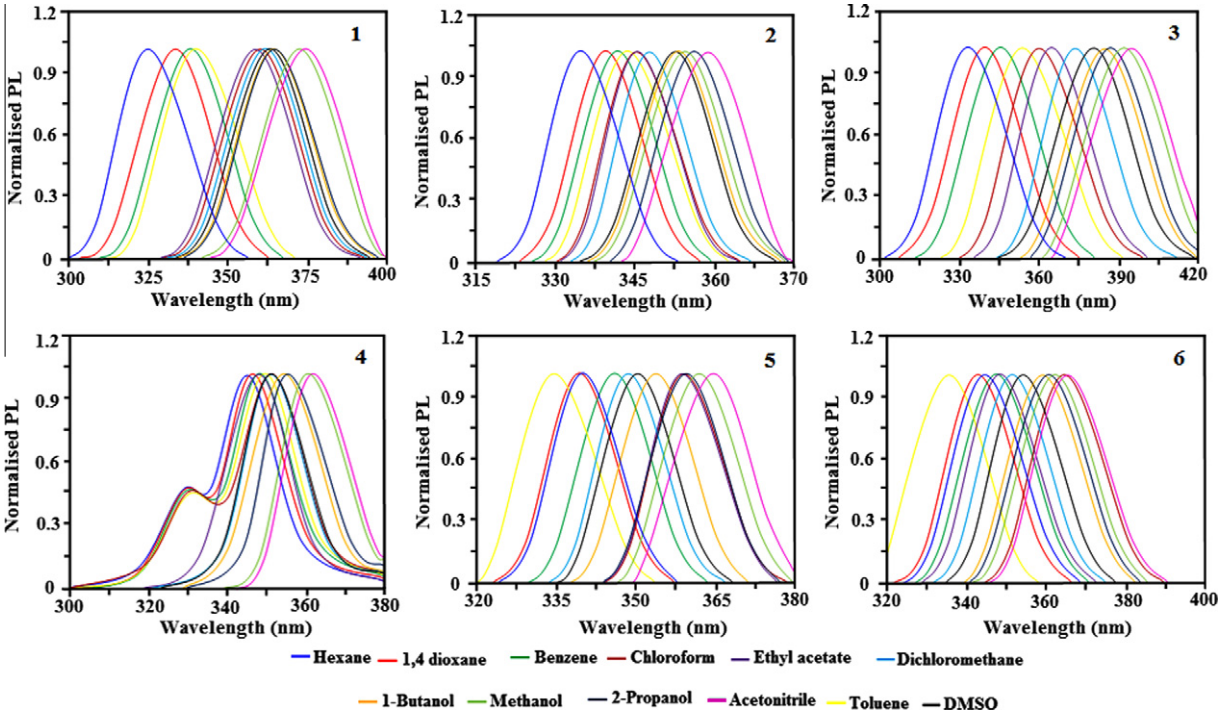

Fig. 3. Emission spectra of the benzimidazole derivatives **1**–**6**.

12.97 ppm in the ^{1}H NMR which is a typical signal for hydrogen bonded hydrogen atom. In order to reveal the contribution of the intramolecular hydrogen bonding in hydroxy benzimidazole **4** to their optical properties, the fluorescence spectra of **4** and its methoxy derivative **6** in dioxane solvent under identical condition (Fig. 5) have been measured. A dual fluorescence detected for **4** with emission peaks centered at 346.8 and 329.3 nm respectively. The emission peak at shorter wavelength (329.3 nm) is assigned to rotamer I and that at the longer wavelength (346.8 nm) is assigned to rotamer II. Whereas compound **6** exhibits emission only at 342.1 nm. The absence of additional peak confirms absence of intramolecular hydrogen bond in **6**. It is further evident that intramolecular hydrogen bonding is the driving force for ESIPT and dual fluorescence behavior of hydroxy benzimidazole derivative **4**.

Table 1
Absorption and emission spectral data of **1–6** in various solvents.

Solvent	Absorption[a] (l, nm)						Emission[b] (l, nm)					
	1	**2**	**3**	**4**	**5**	**6**	**1**	**2**	**3**	**4**	**5**	**6**
Hexane	293.5	292	294.7	296.4	295.7	297.7	323	335.2	333.5	328.6(sh), 345.5	340.6	344.6
1,4-Dioxane	292.9	290.6	294.1	295.6	294.7	296.7	333.1	339.4	337.9	329.3(sh), 346.8	339.3	342.1
Benzene	292.7	290	293.1	292.2	293.7	294.7	338.1	341.4	346.6	329.7(sh), 347.5	346.7	346.9
Toluene	291.2	292.7	292	293.3	294.1	296.1	339.5	343.1	353.5	330.6(sh), 348.4	334.6	334.2
Chloroform	291.7	289	291.7	292.5	293	293.7	358.9	346.6	360.1	331.7(sh), 349.9	360.7	364.9
Ethyl acetate	290	290.7	288.7	293.9	292.7	295.7	357.6	346	365.7	347.7	358.9	347.7
Dichloromethane	289.9	291.6	277.6	293.7	292.7	294.1	361.7	347.9	373.7	351.6	348.6	351.6
DMSO	289.7	289.7	273	292.5	290.5	293.7	363.2	353.1	381.6	351.7	351.3	354.4
1-Butanol	287.5	288.8	263.5	292.6	291.6	292.7	365.5	354.6	385.8	353.4	353.4	359.8
2-Propanal	291.4	287.7	261.4	291.4	290.6	291.7	364.6	356.2	387.5	355.3	357.7	361.1
Methanol	286.9	289.7	283.6	289.6	288.6	289.7	370.9	354.8	391.8	359.7	359.7	363.7
Acetonitrile	288.5	283.6	273.7	288.5	287.5	289.1	373	357.1	393.8	362.6	363.7	366.6

[a] Solution concentration = 1×10^{-5} M.
[b] Solution concentration = 1×10^{-8} M.

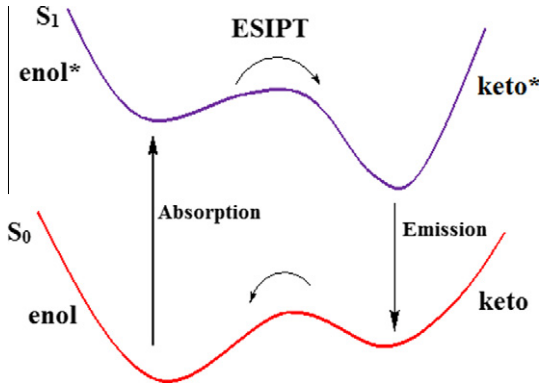

Fig. 4. ESIPT mechanism of the benzimidazole derivative **4**.

Table 2
Electron density of atoms N(15) oxygen of **4**.

Atom	II	II[a]	III
N(15)	−0.397	−0.458	0.315
O(35)	−0.572	−0.529	−0.699

[a] Corresponds to excited state.

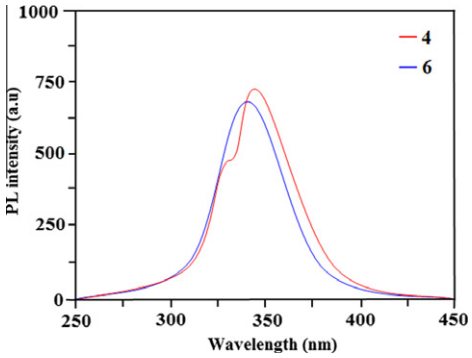

Fig. 5. Fluorescence spectra of the benzimidazole derivatives **4** and **6** in dioxane.

Evidence for ESIPT

In the present study, theoretical calculations have been used to support ESIPT process [33–35]. The ground-state geometries of three species, I and II of **4** have been optimized using DFT/B3LYP/6-31G(d,p) method. The energies of excited state have also been calculated using standard CIS method. Table 3 gives the energies and dipole moment of the species I and II in the ground and the excited states.

Table 3
Relative energies and dipole moment of **4**.

Rotamer	Ground state		Excited state	
	μ (D)	E (eV)	μ (D)	E (eV)
I	4.85	0.07 (0.00)	9.23	4.02 (3.50)
II	4.57	0.08 (0.03)	9.02	4.54 (4.01)

In the excited state the azomethine nitrogen atom becomes richer in electrons than the hydroxylic oxygen atom. The π-electron densities in the excited state are the driving force for the intramolecular proton transfer from the hydroxylic group to the azomethine nitrogen atom. The potential energy surface (PES) curves (Fig. 6a and b) for the interconversion of isomers I and II of **4** in the ground state for isolated molecule is 4.6 kcal/mol and that in ethanol is 3.7 kcal/mol. The corresponding value in the excited state for the isolated molecule is 12.7 kcal/mol and that in ethanol is 10.1 kcal/mol, respectively. The barrier for interconversion in the excited state is much higher than that in the ground state.

Competition of intra and intermolecular hydrogen bonding in binary solvents

The competition of intra and intermolecular hydrogen bonding in **4** has been studied in dioxane–water mixture. In pure dioxane, hydroxy benzimidazole **4** exhibits both normal and tautomer emission at 329.3 and 346.8 nm respectively. The tautomer emission intensity decreases relatively to that of the normal emission with the addition of water. When water fraction is increased to 20% (v/v), the tautomer emission almost vanished. With further increasing water fraction to 40% (v/v), a new emission band appeared at 337.5 nm in addition to the normal emission. This band intensity increased with increasing water fraction and turned to the main emission when water fraction is 80% (v/v) (Fig. 7). It shows that the tautomer emission decreases with increasing water fraction in the mixed solvent if the intermolecular hydrogen bonding between **4** and water is taken into account. In the initial stage, presence of small amount of water in dioxane solution must give rise to solvation of **4**. The intermolecular hydrogen bonding between **4** and water definitely disrupts the ground state

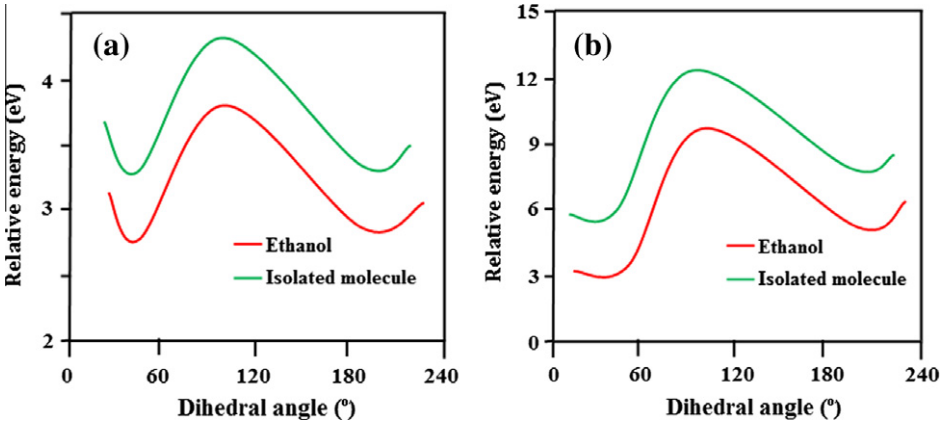

Fig. 6. The potential energy surface curves for the interconversion of isomers I and II of the benzimidazole derivative **4** in the ground and excited states.

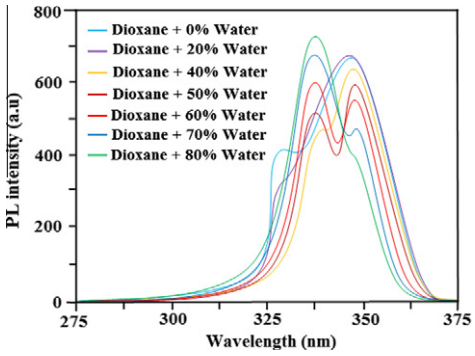

Fig. 7. Competition of intra and intermolecular hydrogen bonding of the benzimidazole derivative **4** in binary solvents.

intramolecular hydrogen bonding rotamers I and II but increases the quantity of species III, in which ESIPT and tautomer formation are inhibited. Consequently the tautomer emission decreases with addition of water and finally vanished [36].

HOMO–LUMO energies of benzimidazole derivative by DFT method

Analysis of the electron density of HOMO and LUMO (Fig. S2) of **4** can through some light on the ground and excited states proton transfer processes. HOMO of enol form predicts that intramolecular hydrogen bonded (IMHB) ring system posses bonding character over the O(35) H(39) and C(10) C(8) atoms, where as C(7) is antibonding character. Both the hydroxyl oxygen [O(35)] and nitrogen [N(15)] have bonding character, with a larger electron density over the hydroxyl oxygen(O(35)). Electron density of HOMO of keto tautomer around IMHB ring shows antibonding character over the H(36) O(37), O(3) C(5) and N(15) H(36) atoms and bonding character over the C(10) C(8) C(7) atoms. Again comparison of HOMO of enol form with HOMO of keto form shows much larger electron density on O(35). In the later case HOMO electron density for both the enol and keto form shows less electron density over the phenyl ring.

By considering LUMO of enol and keto forms, LUMO of the enol tautomer possess high electron density on O(35). After tautomerization, LUMO of keto-tautomer still shows larger electron density on N(15) and comparatively smaller density on O(35). Thus it favors the transfer of a proton from O(35) to N(15) in the excited state (ESIPT). Again our calculation of electron density over the proton transfer co-ordinate in the excited states (i.e., LUMO electron densities) show that there is a shift of p-electron distribution from O(35) to N(15). Analysis of electron density of HOMO for enol tautomer predicts N(15) has slightly higher bonding character than O(35). On the other hand, HOMO electron density of keto tautomer shows greater bonding character of O(35) than N(15) and hence transfer of proton from O(35) to N(15) in the ground state (ESIPT) is quite impossible.

Crystal structure

Crystalline benzimidazole derivative (**5**) [37] are triclinic crystal. It crystallizes in the space group $P\bar{1}$. The cell dimensions are a = 9.6610 Å, b = 10.2900 Å, and c = 17.7271 Å. ORTEP diagram of (**5**) (Fig. S3) shows that the benzimidazole ring is essentially planar. The dihedral angles between the planes of the benzimidazole and the benzene rings of the 4-methylbenzyl and the *p*-tolyl groups are 76.64(3)° and 46.87(4)°, respectively, in molecule A. The corresponding values in molecule B are 86.31(2)° and 39.14(4)°. The dihedral angle between the planes of the two benzene rings is 73.73(3)° and 80.69(4)° in molecules A and B, respectively. Optimization of **5** have been performed by DFT at B3LYP/6-31G(d,p) using Gaussian-03. All these XRD data are in good agreement with the theoretical values (Table 4). However, from the theoretical values it can be found that most of the optimized bond lengths, bond angles and dihedral angles are slightly higher than that of XRD values. These deviations can be attributed to the fact that the theoretical calculations were aimed at the isolated molecule in the gaseous phase and the XRD results were aimed at the molecule in the solid state.

Conclusion

Intermolecular hydrogen bonding of hydroxy benzimidazole derivative with water giving rise to III inhibits the ESIPT process, resulting in an increase in the quantum yield of normal emission at the expense of the tautomer emission. Electron density and HOMO–LUMO analysis supports the ESIPT process in hydroxy benzimidazole derivative. Analysis of HOMO, LUMO π-electron density shows that the electron density on the hydroxyl oxygen (O(35)) is quite high compare to the N(15) of the enol tautomer. Again, after the transfer of proton along the proton transfer co-ordinate shows the same oxygen atom, i.e., (O(35)) has higher electron density than N(15) in the keto form. This explained the non-viability of ground state electron transfer. On the other hand, the LUMO electron density shows a drift of electron cloud from O(35) to N(15) along the proton transfer co-ordinate and explaining the viability of ESIPT process. The potential energy surface curves for the interconversion of isomers I and II of **4** shows the

Table 4
Selected bond lengths (Å), bond angles (°) and torsional angles (°) of **5**.

Bond lengths (Å)	Experimental XRD (Å)	Bond angles (°)	Experimental XRD (°)	Torsional angles (°)	Experimental XRD (°)
N1A–C2A	1.3782(1.4972)	C2A–N1A–C8A	106.23(101.69)	C2A–N1A–C1A–C11A	109.45(−177.75)
N1A–C8A	1.3833(1.4584)	C2A–N1A–C1A	128.33(113.71)	C8A–N1A–C1A–C11A	−81.12(−62.25)
N1A–C1A	1.4537(1.4700)	C8A–N1A–C1A	124.79(113.33)	C9A–N3A–C2A–N1A	−0.02(−13.69)
N3A–C2A	1.3163(1.3671)	C2A–N3A–C9A	104.77(105.49)	C9A–N3A–C2A–C21A	−178.71(165.91)
N3A–C9A	1.3881(1.4606)	C2B–N1B–C8B	106.27(101.69)	C8A–N1A–C2A–N3A	0.59(17.54)
N1B–C2B	1.3795(1.4972)	C2B–N1B–C1B	129.32(113.71)	C1A–N1A–C2A–N3A	171.55(139.72)
N1B–C8B	1.3863(1.4584)	C8B–N1B–C1B	123.98(113.33)	C8A–N1A–C2A–C21A	179.28(−162.06)
N1B–C1B	1.4550(1.4700)	C2B–N3B–C9B	105.12(105.41)	C1A–N1A–C2A–C21A	−9.75(−39.88)
N3B–C2B	1.3174(1.3671)	N1A–C1A–C11A	115.07(109.47)	C9A–C4A–C5A–C6A	0.1(−0.1581)
N3B–C9B	1.3866(1.4606)	N3A–C2A–N1A	113.25(113.53)	C2A–N1A–C8A–C7A	178.45(166.15)
C1A–C11A	1.5135(1.5400)	N3A–C2A–C21A	123.44(123.23)	C1A–N1A–C8A–C7A	7.08(43.71)
C2A–C21A	1.4729(1.5400)	N1A–C2A–C21A	123.30(123.24)	C2A–N1A–C8A–C9A	−0.88(13.70)
C7A–C8A	1.3921(1.3862)	N1A–C8A–C3A	131.76(130.72)	C1A–N1A–C8A–C9A	−172.25(136.15)
C8A–C9A	1.3999(1.4763)	N1A–C8A–C9A	103.49(108.25)	C6A–C7A–C8A–N1A	179.75(176.19)
C14A–C17A	1.5089(1.5400)	N3A–C9A–C4A	129.91(130.69)	C2B–N1B–C1B–C11B	108.10(−177.75)
C24A–C27A	1.5078(1.5400)	N3A–C9A–C8A	110.26(108.25)	C8B–N1B–C1B–C11B	−79.66(−62.25)
				C9B–N3B–C2B–N1B	−0.86(−13.69)
				C9B–N3B–C2B–C21B	177.35(165.91)
				C8B–N1B–C2B–N3B	1.24(17.54)
				C1B–N1B–C2B–N3B	173.85(139.72)
				C8B–N1B–C2B–C21B	−176.90(162.06)
				C1B–N1B–C2B–C21B	−4.29(−39.88)
				C9B–C4B–C5B–C6B	0.25(−0.1581)
				C2B–N1B–C8B–C7B	176.39(166.15)
				C1B–N1B–C8B–C7B	3.28(43.71)
				C2B–N1B–C8B–C9B	−1.05(−13.70)
				C1B–N1B–C8B–C9B	−174.15(−136.15)
				C6B–C7B–C8B–N1B	177.76(176.19)

Values within the parenthesis corresponds to theoretical values.

barrier for interconversion in the excited state is much higher than that in the ground state.

Acknowledgments

One of the authors Prof. J. Jayabharathi is thankful to DST (No. SR/S1/IC-73/2010) and DRDO (NRB-213/MAT/10-11) for providing funds to this research study. Mr. K. Jayamoorthy is thankful to DST (No. SR/S1/IC-73/2010) for providing fellowship.

Appendix A. Supplementary material

Supplementary data associated with this article can be found, in the online version, at http://dx.doi.org/10.1016/j.saa.2012.12.037.

References

[1] W.S. Hung, J.T. Lin, C.H. Chien, Y.T. Tao, S.S. Sun, Y.S. Wen, Chem. Mater. 16 (2004) 2480–2488.
[2] K. Nakashima, Biomed. Chromatogr. 17 (2003) 83–95.
[3] E.M. Across, K.M. White, R.S. Moshrefzadeh, C.V. Francis, Macromolecules 28 (1995) 2526–2532.
[4] P.W. Erhardt, J. Med. Chem. 30 (1987) 231–237.
[5] G.L. Gravalt, B.C. Baguley, W.R. Wilson, W.A. Denny, J. Med. Chem. 37 (1994) 4338–4345.
[6] K.J. Soderlind, B. Gorodetsky, A.K. Singh, N. Bachur, G.G. Miller, J.W. Loun, Anticancer Drug Des. 14 (1999) 19–25.
[7] J. Jayabharathi, V. Thanikachalam, K. Jayamoorthy, J. Photochem. Photobiol. B doi: http://dx.doi.org/10.1016/j.jphotobiol.2012.06.014.
[8] T. Roth, M.L. Morningstar, P.L. Boyer, S.H. Hughes, R.W. Buckheit Jr., C.J. Michejda, J. Med. Chem. 40 (1997) 4199–4207.
[9] Y. Bai, J. Lu, Z. Shi, B. Yang, Synlett 12 (2001) 544–546.
[10] E. Hasegawa, A. Yoneoka, K. Suzuki, T. Kato, T. Kitazume, K. Yangi, Tetrahedron 55 (1999) 12957–12968.
[11] E. Bouwman, W.L. Driessen, J. Reedjik, Coord. Chem. Rev. 104 (1990) 143–172.
[12] M.A. Pujar, T.D. Bharamgoudar, Transition Met. Chem. 13 (1988) 423–425.
[13] J. Jayabharathi, V. Thanikachalam, K. Jayamoorthy, Spectrochim. Acta Part A Mol. Biomol. Spectrosc. 89 (2012) 168–176.
[14] L.G. Arnaut, S.J. Formosinho, J. Photchem. Photobiol. A 75 (1993) 1.
[15] J. Jayabharathi, V. Thanikachalam, M. Vennila, K. Jayamoorthy, Spectrochim. Acta A. 95 (2012) 589–595.
[16] J. Jayabharathi, V. Thanikachalam, M. Vennila, K. Jayamoorthy, Spectrochim. Acta A. 95 (2012) 446–451.
[17] A. Douhal, Science 276 (1997) 221–222.
[18] P.T. Chou, M.L. Martinez, J.H. Clements, J. Phys. Chem. 97 (1993) 2618–2622.
[19] L.F. Campo, F.S. Rodembusch, V. Stefani, J. Appl. Polym. Sci. 99 (2006) 2109–2116.
[20] Y. Wu, X. Peng, J. Fan, S. Gao, M. Tian, J. Zhao, S. Sun, J. Org. Chem. 72 (2007) 62–66.
[21] S. Park, O.H. Kwon, Y.S. Lee, D.J. Jang, S.Y. Park, J. Phys. Chem. A 111 (2007) 9649–9653.
[22] S. Park, J. Seo, S.H. Kim, S.Y. Park, Adv. Funct. Mater. 18 (2008) 726–731.
[23] K. Das, N. Sarkar, A.K. Ghosh, D. Majumdar, D.N. Nath, K. Bhattacharyya, J. Phys. Chem. 98 (1994) 9126–9132.
[24] J. Catalan, J.C. Del Valle, J. Am. Chem. Soc. 115 (1993) 4321–4325.
[25] A.U. Khan, M. Kasha, Proc. Natl. Acad. Sci. USA 91 (1994) 8627–8630.
[26] R.W. Munn, Harvard Environ. Law Rev. (1989) 517–533.
[27] F. Vollmer, W. Rettig, J. Photochem. Photobiol., A 95 (1996) 143–155.
[28] A. Sytnik, M. Kasha, Proc. Natl. Acad. Sci. USA 91 (1994) 8627–8630.
[29] S.K. Das, S.K. Dogra, J. Colloid Int. Sci. 205 (1998) 443–453.
[30] I. Lopez Arbeloa, J. Photochem. 14 (1980) 97–105.
[31] J. Jayabharathi, V. Thanikachalam, M. Venkatesh Perumal, N. Srinivasan, Spectrochim. Acta A. 83 (2011) 200–206.
[32] J. Jayabharathi, V. Thanikachalam, K. Saravanan, M. Venkatesh Perumal, Spectrochim. Acta A. 79 (2011) 1240–1246.
[33] P.F. Barbara, P.K. Walsh, L.E. Brus, J. Phys. Chem. 93 (1989) 29–34.
[34] G.J. Woolfe, M. Melzig, S. Schneider, F. Dorr, Chem. Phys. 77 (1983) 213–221.
[35] A.L. Sobolewski, Chem. Phys. Lett. 211 (1993) 293–299.
[36] K. Das, N. Sarkar, D. Majumdar, A.K. Ghosh, D.N. Nath, K. Bhattacharyya, J. Phys. Chem. 98 (1994) 9126–9132.
[37] S. Rosepriya, A. Thiruvalluvar, K. Jayamoorthy, J. Jayabharathi, Antony Linden, Acta Cryst. E67 (2011) o3519.